2007 International Symposium on Nonlinear Theory and its Applications
NOLTA'07, Vancouver, Canada, September 16-19, 2007

Bifurcation of Simple Switched Dynamical Systems based on Power Converters

Yasuhide Ishige†, Yuki Ishikawa† and Toshimichi Saito†

†EECE Dept., HOSEI University, Tokyo, 184-0002 Japan
Email: yasuhide@nonlinear.k.hosei.ac.jp, ishikawa@nonlinear.k.hosei.ac.jp and tsaito@k.hosei.ac.jp

Abstract—This paper studies nonlinear dynamics of basic dc-dc and ac-dc converters in current mode control. In order to avoid the model becoming too complex, we make the simplifying assumption that voltage regulation is achieved in high frequency modulation and the much slower dynamics of output side can be represented by a constant voltage source. Under this assumption we can derive the 1D return map that describes switching phase of the converters. The map enables us to analyze the dynamics precisely. Typical periodic/chaotic phenomena and related bifurcation phenomena are demonstrated.

1. Introduction

Switching power converters are important objects to analyze nonlinear dynamics and have been studied extensively [1]-[2]. The nonlinear switching can cause a variety of chaos and bifurcation phenomena. Analysis of the phenomena is basic to develop novel bifurcation theory and to design efficient circuits. However, systematic analysis is not easy because of complex nonlinearity. This paper studies nonlinear dynamics of basic dc-dc and ac-dc converters [3] - [8] through 1D return maps of switching phase. In such power converters, various switching logics are available and most popular among them are the voltage mode control (VMC) and the current mode control (CMC). This paper studies CMC that is used for achieving faster transient response in boost converters and for lower voltages with higher current capabilities by current sharing in parallel converters [9]. Also, the CMC can be a key to cause a variety of nonlinear phenomena [1], [2].

First, we introduce basic dc-dc boost converters in CMC. In order to avoid the model becoming too complex, we make the simplifying assumption that voltage regulation is achieved in high frequency modulation, so that the much slower dynamics of the outer voltage loop can be ignored, and the output side can be represented by a constant voltage source [3] [5]. Under this assumption we derive a very simple model having piecewise constant (PWC) vector field and piecewise linear (PWL) solutions. From the PWC model we can derive the 1D return map of switching phase. The map is given by an explicit PWL formula and enables us to analyze chaos and bifurcation phenomena precisely. Second, we introduce basic ac-dc converters in CMC. Applying simplifying assumption as the dc-dc converters, we can derive 1D return map of an implicit form based on exact piecewise solution. Using the map we can investigate rich periodic and chaotic phenomena and related bifurcation phenomena.

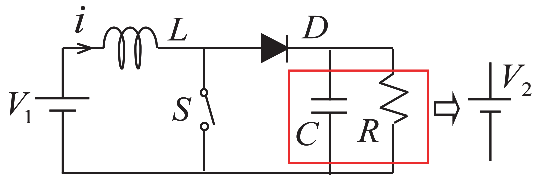

Figure 1: DC-DC boost converter and PWC model.

It should be noted that the 1D return map is available not only for dc-dc and ac-dc boost converters but also for a variety of switching circuits including delta modulator for PWM control [10]. Analysis results of this paper is important not only as basic study but also for practical applications. For example, the results provide basic information to realize stable operation, distortion removal [7] and EMI improvement [4].

2. DC-DC Boost Converters

Fig. 1 shows a basic dc-dc boost converter with CMC switching. The voltage regulation is assumed to be achieved in high frequency modulation, enabling us to analyze only the dynamics of the inner current loop. Under the CMC, when the switch is on, the inductor current i rises, and when it reaches a reference value $I_{\rm ref}$, the switch S is turned off. When S is off D turns on, and the inductor current decays. It is turned on by the arrival of the next rising edge of a free running clock signal of period T. While the switch is off, if the inductor current decays to zero, the system enters the third state in which both S and D do not conduct. Thus there can be three possible states:

State 1: S conducting, D blocking and $0 < i < I_{\rm ref}$
State 2: S blocking, D conducting and $0 < i < I_{\rm ref}$
State 3: S and D both blocking and $i = 0$

The switching rules are:

State 1 $\longrightarrow$ State 2: when $i = I_{\rm ref}$
State 2 $\longrightarrow$ State 3: when $i = 0$
State 2 or State 3 $\longrightarrow$ State 1: when $t = nT$

If the operation of the converter includes State 3, it is said to be in DCM, otherwise it is said to be operating in CCM. As stated earlier, we make the simplifying assumption that $T << RC$ and voltage regulation is achieved. In this case we can replace the RC with the constant voltage source V_2.

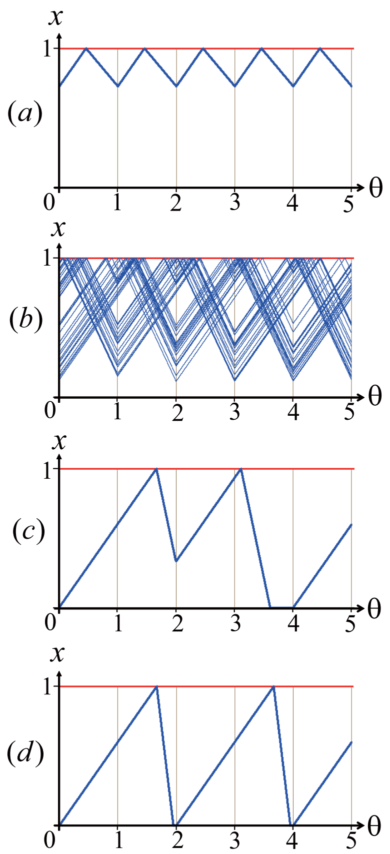

Figure 2: Typical waveforms for $a = 0.6$. (a) periodic behavior in CCM for $b = 0.5$, (b) chaotic behavior for $b = 0.9$ (overwritten), (c) periodic behavior in DCM for $b = 2.0$, (d) periodic behavior in DCM for $b = 3.5$

Thus the circuit equation becomes

$$L\frac{d}{dt}i = \begin{cases} V_1 & \text{for State 1} \\ -(V_2 - V_1) & \text{for State 2} \\ 0 & \text{for State 3} \end{cases} \tag{1}$$

where $0 < V_1 < V_2$ and all the circuit elements are assumed to be ideal. This is the PWC model having PWL solutions. We introduce the dimensionless variables and parameters

$$\tau = \frac{t}{T}, \quad x = \frac{i}{I_{\mathrm{ref}}}, \quad a = \frac{TV_1}{LI_{\mathrm{ref}}}, \quad b = \frac{T(V_2 - V_1)}{LI_{\mathrm{ref}}} \tag{2}$$

through which Eq. (1) is transformed into

$$\frac{d}{d\tau}x = \begin{cases} a & \text{for State 1} \\ -b & \text{for State 2} \\ 0 & \text{for State 3} \end{cases}, \quad a > 0,\ b > 0 \tag{3}$$

and the switching rules become

$$\begin{array}{ll} \text{State 1} \longrightarrow \text{State 2} & \text{if } x = 1 \\ \text{State 2} \longrightarrow \text{State 3} & \text{if } x = 0 \\ \text{State 2 or 3} \longrightarrow \text{State 1} & \text{if } \tau = n \end{array}$$

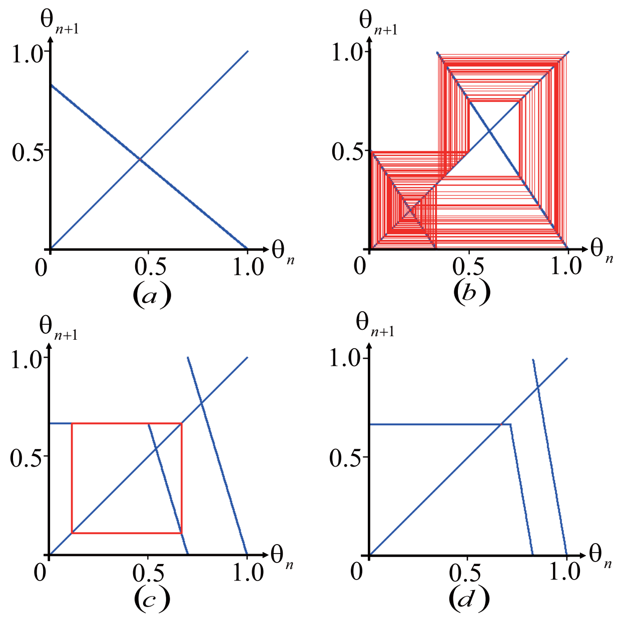

Figure 3: Return maps for $a = 0.6$. (a) periodic orbit for $b = 0.5$, (b) chaos for $b = 0.9$ (overwritten), (c) SSPO with period 2 for $b = 2.0$, (d) SSPO with period 1 for $b = 3.5$.

Note that the original five parameters $(T, L, I_{\mathrm{ref}}, V_1, V_2)$ of the PWC model are integrated into the dimensionless two parameters a and b of Eq.(3). Fig. 2 (a) shows typical periodic behavior in CCM. As the parameter b increases, this periodic phenomenon is changed to be chaotic as shown in Fig. 2 (b). As the parameter b increases further, the system becomes to operate in DCM as shown in Fig. 2 (c) and (d). In the DCM a variety of periodic behavior appears.

We now derive 1D return map. Let τ_n denote n-th switching moment at which x reaches the threshold 1 and State 1 is changed into State2. Since τ_{n+1} is determined by τ_n we can define 1D map of the form $\tau_{n+1} = f(\tau_n)$. Since the system is peiod 1, we introduce phase variable $\theta_n = \tau_n$ mod 1 and the map can be reduced into the return map from $I \equiv [0, 1)$ to itself: $\theta_{n+1} = F(\theta_n) = f(\theta_n)$ mod 1. When a trajectory starts from $x = 1$ at time τ_n and returns $x = 1$ at time τ_{n+1}, there are two possibilities; Type 1: x does not reach $x = 0$ and Type 2: x reaches $x = 0$. If $b > 1$ these two types exist and the map is described by

$$f(\theta_n) = \begin{cases} -p(\theta_n - 1) + 1 & \text{for } \theta_a < \theta_n \leq 1 \\ a^{-1} + 1 & \text{for } 0 < \theta_n \leq \theta_a \end{cases} \tag{4}$$

where $p \equiv b/a$ and $\theta_a \equiv 1 - b^{-1}$. If $0 < b < 1$, Type 2 does not exist hence the second branch with zero-slope does not exist. It should be noted that the return map F of phase θ is simpler than return map of state variables in [5].

Fig. 3 shows typical examples of the return map. If $a > b$ the return map has contracting slope $|p| < 1$ and exhibits stable periodic orbit as shown in Fig. 3(a) [1]. If $a < b < 1$

[1] Definition of stable periodic orbits can be found in [5]

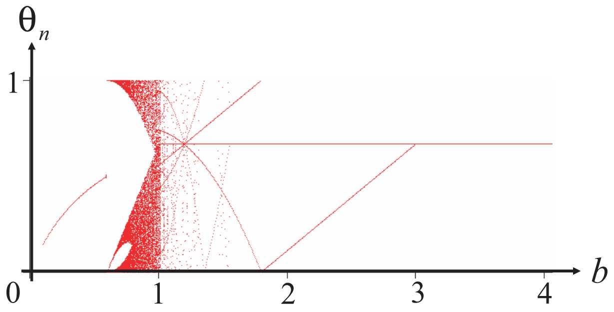

Figure 4: Bifurcation diagram for $a = 0.6$.

the map has expanding slope $|p| > 1$ and exhibits chaos as shown in Fig. 3(b). If $b > 1$ the map has zero-slope and exhibits superstable periodic orbits (SSPOs) as shown in Fig. 3(c) and (d). They correspond to periodic behavior in DCM (Fig. 2 (c) and (d)). These phenomena are summarized in the bifurcation diagram in Fig. 4.

3. AC-DC Boost Converters

Fig. 5 shows a basic ac-dc boost converter with CMC switching. The input $v_1(t) = V_1|\sin\frac{\pi}{mT}t|$ is an output of rectifier where T is period of the clock signal and m is a positive integer. The rectifier is omitted in the figure. In this circuit, the reference value is not dc but has component proportional to the input: $I_{\rm ref}(t) = kv_1(t) + I_2$. Under the CMC, the possible states of switches are given by replacing $I_{\rm ref}$ for dc-dc converters with $I_{\rm ref}(t)$.

State 1: S conducting, D blocking and $0 < i < I_{\rm ref}(t)$
State 2: S blocking, D conducting and $0 < i < I_{\rm ref}(t)$
State 3: S and D both blocking and $i = 0$

The switching rules are:

State 1 $\longrightarrow$ State 2: when $i = I_{\rm ref}(t)$
State 2 $\longrightarrow$ State 3: when $i = 0$
State 2 or State 3 $\longrightarrow$ State 1: when $t = nT$

The output voltage regulation is assumed to be achieved in high frequency modulation as the dc-dc converters. Applying this assumption ($T << RC$), the RC can be replaced with the constant voltage source V_2. Thus the circuit equation becomes

$$L\frac{d}{dt}i = \begin{cases} v_1(t) & \text{for State 1} \\ v_1(t) - V_2 & \text{for State 2} \\ 0 & \text{for State 3} \end{cases} \qquad (5)$$

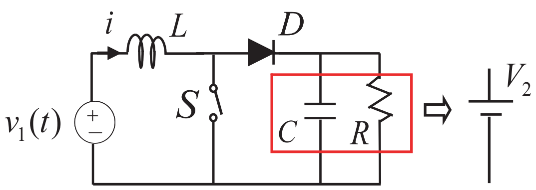

Figure 5: AC-DC boost converter and PWC model.

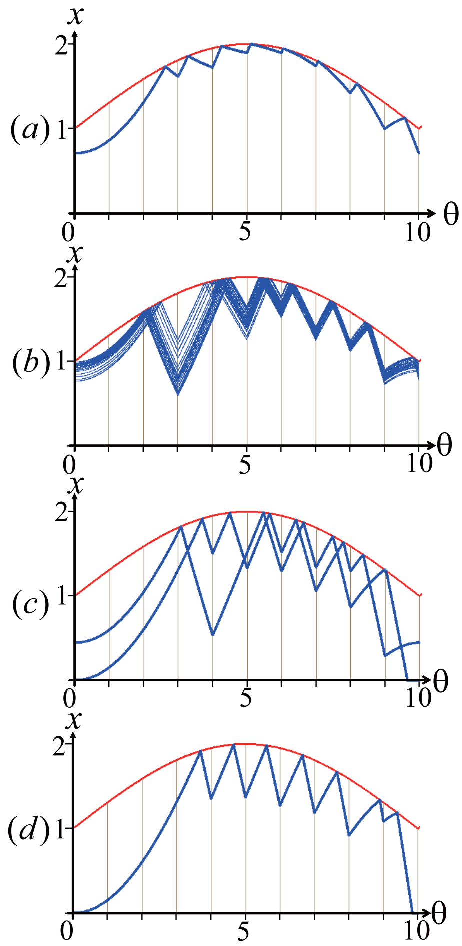

Figure 6: Typical waveforms for $\alpha = 1$, $\gamma = 1$ and $m = 10$. (a) periodic behavior in CCM for $\beta = 1.1$, (b) chaotic behavior for $\beta = 1.7$ (overwritten), (c) periodic behavior in DCM for $\beta = 2.3$, (d) periodic behavior in DCM for $\beta = 2.8$.

where $0 < v_1(t) < V_2$. We introduce the dimensionless variables and parameters

$$x = \frac{i}{kV_1},\ \tau = \frac{t}{T},\ \alpha = \frac{T}{Lk},\ \beta = \frac{TV_2}{LkV_1},\ \gamma = \frac{I_2}{kV_1} \qquad (6)$$

through which Eq. (5) is transformed into

$$\frac{d}{d\tau}x = \begin{cases} \alpha s(\tau) & \text{for State 1} \\ \alpha s(\tau) - \beta & \text{for State 2} \\ 0 & \text{for State 3} \end{cases} \qquad (7)$$

where $s(\tau) = |\sin\frac{\pi}{m}\tau|$.

State 1 $\rightarrow$ State 2 if $x = s(\tau) + \gamma$
State 2 $\rightarrow$ State 3 if $x = 0$
State 2 or State 3 $\rightarrow$ State 1 if $\tau = n$

Fig. 6 (a) shows typical periodic waveform in CCM. As the parameter β increases, this periodic behavior is changed into chaotic behavior as shown in Fig. 6 (b) and then to periodic behavior in DCM as shown in Fig. 6 (c) and (d).

We derive the 1D return map in a similar manner to the dc-dc converters. Let τ_n denote n-th switching moment at which x reaches the threshold and State 1 is changed into State2. Since τ_{n+1} is determined by τ_n we can define 1D map of the form $\tau_{n+1} = f(\tau_n)$. Since the system is period m, we introduce phase variable $\theta_n = \tau_n$ mod m and the map can be reduced into the return map from $I_m \equiv [0, m)$ to itself: $\theta_{n+1} = F(\theta_n) = f(\theta_n)$ mod m.

Fig. 7 (a) shows a return map of a stable periodic orbit corresponding to periodic behavior in CCM in Fig. 6 (a). As β increases, the return map lost stability and the periodic orbit is changed into chaotic orbit in CCM as shown in Fig. 7(b). As β increases further, zero-slope appears in the map and we can observe rich SSPOs as shown in Fig. 7 (c) and (d). They correspond to periodic behavior in DCM in Fig. 6 (c) and (d). These phenomena are summarized in the bifurcation diagram in Fig. 8. Such complex behavior relate deeply to undesired operation such as current distortion.

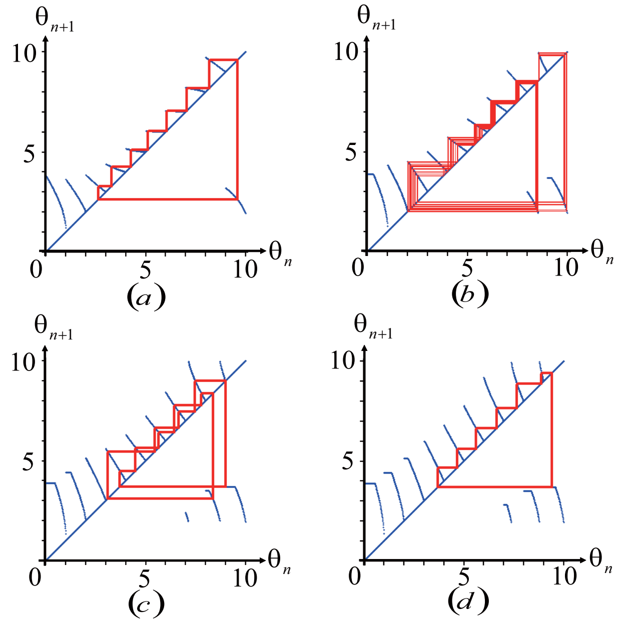

Figure 7: Return maps for $\alpha = 1$ and $\gamma = 1$. (a) periodic orbit for $\beta = 1.1$, (b) chaos for $\beta = 1.7$ (overwritten), (c) SSPO with period 2 for $\beta = 2.3$, (d) SSPO with period 1 for $\beta = 2.8$

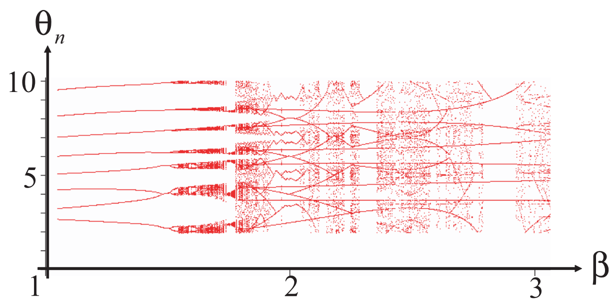

Figure 8: Typical bifurcation phenomena for $\alpha = 1.0$ and $\gamma = 1$.

4. Conclusions

Nonlinear dynamics of basic dc-dc and ac-dc converters has been studied in this paper. In order to realize precise analysis, we make the simplifying assumption that voltage regulation is achieved in high frequency modulation and derive the 1D return map that describes switching phase of the converters. The map enables us to analyze rich periodic and chaotic phenomena precisely.

Future problems are many, including; detailed analysis of bifurcation phenomena of ac-dc converters, generalization of 1D return map of switching phase and design and experiments of practical circuits.

Acknowledgment

The authors wish to thank Assoc. Prof. Hiroyuki Torikai of Osaka University for his valuable comments.

References

[1] S. Banerjee and G. C. Verghese, eds., Nonlinear Phenomena in Power Electronics: Attractors, Bifurcations, Chaos, and Nonlinear Control, IEEE Press, 2001.

[2] C. K. Tse and M. di Bernardo, Complex behavior in switching power converters, Proc. IEEE, 90, pp. 768-781, 2002.

[3] D. C. Hamill and D. J. Jeffries, " Subharmonics and chaos in a controlled switched-mode power converter, " *IEEE Trans. Circuits Systs. I,* vol.35, pp. 1059-1061, 1988.

[4] J. H. B. Deane and D. C. Hamill, Improvement of power supply EMC by chaos, Electron. Lett. 32, 12, p. 1045, 1996

[5] T. Kabe, S. Parui, H. Torikai, S. Banerjee and T. Saito, Analysis of Current Mode Controlled DC-DC Converters through Piecewise Linear Models, IEICE Trans. Fundamentals, E90-A, 2, pp. 448-456, 2007.

[6] C. K. Tse, O. Dranga and H. H. C. Iu, Bifurcation analysis of a power-factor-correction boost converter: uncovering fast-sscale instability, Proc. IEEE/ISCAS, III, pp. 312-315, 2003.

[7] J. C. P. Liu, C. K. Tse, N. K. Poon, B. M. H. Pong and Y. M. Lai, A PFC voltage regulator with low input current distortion derived from a rectifierless topology, IEEE Trans. Power Electron., 21, 4, pp. 906-911, 2006.

[8] Jose R. Rodriguez, Juan W. Dixon, Jose R. Espinoza, Jorge Pontt, Pablo Lezana, PWM Regenerative Rectifiers: State of the Art, IEEE Trans. Industorial Electronics, pp. 5-22, 2005.

[9] R. Giral, L. Martinez-Salamero and S. Singer, Interleaved converters operation based on CMC, IEEE Trans. Power Electron., 14, 4, pp. 643-652, 1999

[10] H. Shimazu, T. Saito and H. Torikai, Analysis of conventional/improved delta modulators as switched dynamical systems, Proc. IEEE/IECON, pp. 1814-1817, 2003.